

CONFORMATIONS OF TRICYANOFURAN-TYPE METASTABLE-STATE  
PHOTOACIDS

by

JUAN E. ARIAS

A thesis submitted in partial fulfillment of the requirements  
for the Honors in the Major Program in Chemistry  
in the College of Sciences  
and in the Burnett Honors Colleague  
at the University of Central Florida  
Orlando, Florida

Spring Term, 2019

Thesis Chair: Karin Y. Chumbimuni-Torres

## ABSTRACT

Tricyanofuran-type metastable-state photoacids, relative newcomers to the field of photochromism, outperform traditional light-controlled molecular switches in regards to applicability in biological systems. In a preliminary attempt to understand the underlying processes that govern these compounds, this thesis project establishes the isomeric identity of an unsubstituted tricyanofuran-type metastable-state photoacid, referred to as TCF 1 in this work. Two-dimensional nuclear magnetic resonance experiments are employed to experimentally determine the presence and identity of the open-form TCF 1 isomers. Electronic structure calculations are then used to provide quantitative insight into the experimental results. Experiment and theory show that four out of eight possible open-form isomers exist in solution. To validate the information obtained theoretically, the calculation methodologies are tested against experimental chemical shifts. The impressive agreement with the experiments gives credibility to the picture painted by the theoretical models.

## DEDICATIONS

To my family, friends, and mentors. My success is theirs.

## ACKNOWLEDGEMENTS

I would like to express my thanks to Renan Gongora - for showing me the world of chemistry, Parth Patel - for his years of guidance, and to Eduardo Romero - for opening the door of theory to me. Many thanks are also due to Dr. David Richardson for running the 2D NMR experiments and helping me with the interpretation, and to Dr. James Harper for our insightful conversations regarding NMR in the experiments, in theory, and at the interface of the two. Without Dr. Florencio Hernandez, this work would not have been possible; his invaluable contributions to my growth through allowing me to train in his group, guiding me in research and academia, and providing powerful recommendations, have deeply impacted me and shaped my desire to pass it on. Finally, I would like to express my deepest gratitude to Dr. Karin Chumbimuni-Torres for letting me serve in her lab for the past couple of years. Her trust allowed me to pursue this independent research project and her guidance helped me make it into something I am proud of.

# TABLE OF CONTENTS

<b>1</b>	<b>INTRODUCTION</b>	<b>1</b>
1.1	Photochromic compounds . . . . .	1
1.2	Metastable-state photoacids . . . . .	4
1.3	Studying mPAHs with electronic structure . . . . .	7
<b>2</b>	<b>RESOLVING THE ISOMERIC IDENTITY OF TCF 1</b>	<b>8</b>
2.1	Heteronuclear single quantum correlation NMR experiment . . . . .	10
2.2	Heteronuclear multiple bond correlation NMR experiment . . . . .	11
2.3	Nuclear Overhausser effect NMR experiment . . . . .	12
2.4	Appendix for Chapter 2 . . . . .	16
<b>3</b>	<b>ELECTRONIC STRUCTURE CALCULATIONS</b>	<b>21</b>
3.1	Energies and Boltzmann distributions . . . . .	21
3.2	Structural parameters . . . . .	24
3.3	Chemical shieldings . . . . .	26
<b>4</b>	<b>DISCUSSION AND FUTURE WORK</b>	<b>34</b>
<b>5</b>	<b>REFERENCES</b>	<b>39</b>

# LIST OF TABLES

2.1	Information in $^1\text{H}$ NMR spectra for TCF 1 . . . . .	17
2.2	Information in $^{13}\text{C}$ NMR spectra for TCF 1 . . . . .	17
2.3	HSQC and HMBC interactions for TCF 1 . . . . .	20
2.4	NOE interactions for TCF 1 . . . . .	20
3.1	Normalized energies (kJ/mol) for TCF 1 isomers . . . . .	22
3.2	Normalized energies (kJ/mol) for TCF 1 open-protonated forms and transition states, with the corresponding reaction rate constants. . .	24
3.3	Structural parameters for TCF 1 isomers . . . . .	25
3.4	Theoretical vs. experimental chemical shieldings for TCF 1 B3LYP/6- 311++G(2d, p), single molecule. . . . .	29
3.5	Theoretical vs. experimental chemical shieldings for TCF 1 B3LYP/6- 311++G(2d, p), hydrogen-bonding with an explicit DMSO molecule. . .	32
3.6	Theoretical vs. experimental chemical shieldings for TCF 1 MP2/6- 31+G(d, p), single molecule. . . . .	33

# LIST OF FIGURES

1.1	Photochromic reaction . . . . .	1
1.2	Stilbene . . . . .	2
1.3	Azobenzene . . . . .	2
1.4	Traditional spiro compounds . . . . .	2
1.5	Resonance forms for open spiro compounds . . . . .	3
1.6	Merocyanine-type mPAHs . . . . .	5
1.7	Tricyanofuran-type mPAHs . . . . .	5
2.1	Closed enantiomers of TCF 1 . . . . .	9
2.2	Open conformations of TCF 1 . . . . .	9
2.3	HSQC spectra for TCF 1 . . . . .	10
2.4	HMBC spectra for TCF 1 . . . . .	12
2.5	Chemical shieldings for TCF 1 . . . . .	13
2.6	NOE spectra for TCF 1 . . . . .	14
2.7	Relevant NOE interactions observed . . . . .	15
2.8	Full (above) and zoomed-in (below) 1D $^1\text{H}$ NMR for TCF 1 . . . . .	18
2.9	Full (above) and zoomed-in (below) 1D $^{13}\text{C}$ NMR for TCF 1 . . . . .	19
3.1	Labeling scheme for carbons and hydrogen in TCF 1 . . . . .	27

4.1	Cisoid intermediates for TCF 1 . . . . .	36
4.2	Transient absorbance spectra for TCF 1 . . . . .	38



# INTRODUCTION

## 1.1 PHOTOCROMIC COMPOUNDS

Crano and Guglielmetti define organic photochromic compounds as dyes that can undergo a reversible transformation induced by radiation of light, usually in the UV or visible region of the electromagnetic spectrum.<sup>1</sup>

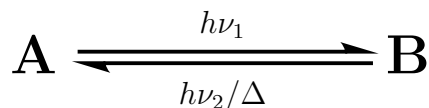


**Figure 1.1:** Photochromic reaction

In the generic case presented in Figure 1, species A photoisomerizes into species B upon radiation of light with energy  $h\nu_1$ . The reverse process, a transformation from B into A, can occur either by radiation of light with different energy  $h\nu_2$  or by thermal relaxation. The forms A and B often differ in their physical properties, such as relative stabilities, boiling and melting points, polarities, and absorbance and emission profiles.

The two conformations of stilbene (*cis* and *trans*) serve to illustrate the profound differences of seemingly small changes in geometry. Fisher et al. determined the *trans* isomer to be more stable than the *cis* by 3.7 Kcal/Mol (methylcyclohexane at 27°C) by comparing their heats of hydrogenation.<sup>2</sup> *Cis*-stilbene has a melting

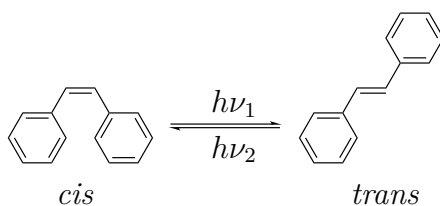


**Figure 1.2:** Stilbene

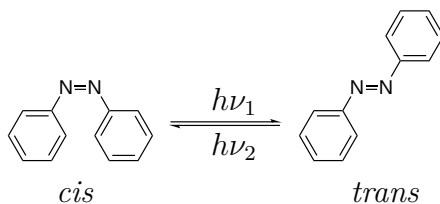


**Figure 1.3:** Azobenzene

point of  $-5^{\circ}\text{C}$  whereas *trans*-stilbene has a melting point of  $123 - 124^{\circ}\text{C}$ .<sup>3, 4</sup>

Azobenzenes are azo analogues of stilbene that feature similar differences in their two isomers. Cembran et al. determined the *trans* isomer of the unsubstituted azobenzene to be more stable than the *cis* isomer by 11.9 - 16.4 Kcal/mol using refined quantum chemistry calculations.<sup>5</sup> The photoisomerization mechanism of azobenzene has been a source of controversy for decades, with the community split between an inversion pathway and a rotation pathway along the nitrogen-nitrogen double bond.<sup>6 - 9</sup>

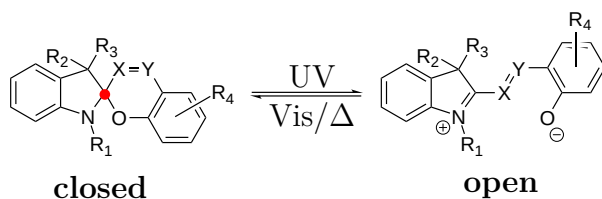


**Figure 1.4:** Traditional spiro compounds

Spiro compounds, such as spiropyrans ( $X = \text{CH}$ ,  $Y = \text{CH}$ ), spirooxazines ( $X = \text{CH}$ ,  $Y = \text{N}$ ), spironaphthoxazines ( $X = \text{CH}$ ,  $Y = \text{N}$ ,  $R_2 = \text{Ph}$ ), spirophenan-

thioxazines ( $X = CH$ ,  $Y = N$ ,  $R_2 = 2Ph$ ), and their derivatives are arguably the most well-studied class of photochromic compounds. The stark structural and electronic differences between the **closed** and **open** form (often referred to as **spiro** and **merocyanine** forms, respectively, but renamed herein to avoid ambiguities further in the manuscript) confer spiro compounds promise as molecular switches<sup>10</sup> for application in ion-detection<sup>11</sup>, polymer functionalization,<sup>12–15</sup> fluorescence modulation,<sup>16, 17</sup> imaging,<sup>18, 19</sup> drug delivery,<sup>20</sup> smart fluids,<sup>21</sup> and selective singlet-oxygen generators.<sup>22</sup>

The closed form has a chiral  $sp^3$  carbon (spiro carbon, labeled with a red dot in Figure 1.4) breaking the conjugation between the indoline and chromene moieties. Thus, in most cases, the electronic excitations of the lowest energy in the closed form consist of transitions localized to the two orthogonal halves<sup>23–25</sup> (several compounds have been designed specifically to allow for charge transfer between the two moieties).<sup>26, 27</sup> The transitions in the spiro compounds lacking charge transfer correspond to energies in the UV region of the electromagnetic spectrum, making the closed form colorless in the visible region. Unless charged substituents are attached to the basic cores, spiro compounds are neutral in their closed form and have a lower dipole moment than their open counterpart.<sup>28, 29</sup>

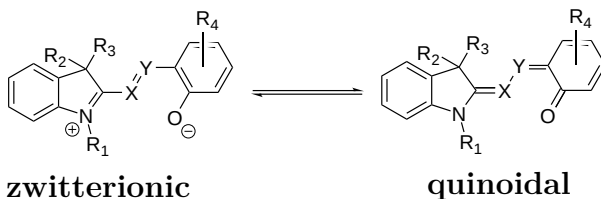


**Figure 1.5:** Resonance forms for open spiro compounds

The planar or semi-planar open form has an extended  $\pi$  framework with electronic excitations in the visible region of the electromagnetic spectrum. The

quinoidal and zwitterionic forms of the open conformer exist in resonance, with the solvent and the nature and location of substituents affecting the relative stability between the quinoidal and zwitterionic resonances (Figure 1.5).<sup>30–32</sup>

In addition to shifting the equilibrium between the resonances of the open form, substituents and solvent can shift the equilibrium between the closed and open forms. For example, polar solvents and electron-withdrawing groups in the chromene moiety tend to stabilize the open form.<sup>33</sup> Not only do solvents and substituents affect the different equilibria at play, they also affect the absorbance profiles and the polarities of both the closed and open forms themselves and the kinetics of the isomerization processes. As a result, one can tailor the behavior of the molecule with appropriate functionalization and choice of solvent.

For more information on the properties and applications of traditional spiro compounds, the interested reader is referred to Mink’s and Klan’s reviews, respectively.<sup>33, 34</sup>

## 1.2 METASTABLE-STATE PHOTOACIDS

Metastable-state photoacids (mPAHs), a relatively new family of spiro compounds, have several characteristics that makes them attractive for use as molecular switches over their traditional counterparts. Liao was the first to report the two known mPAH cores: the merocyanine (*Mer*) core<sup>35</sup> and the tricyanofuran (TCF) core.<sup>36</sup> *Mer*-mPAHs are protonated spiropyrans that stabilize the open form in a zwitterionic fashion with an N-alkyl sulfonate group that counterbalances the positive charge on the indoline nitrogen. TCF mPAHs replace the indoline moiety altogether with a tricyanofuran moiety. The TCF mPAHs reported up to date are also more stable in their open form.

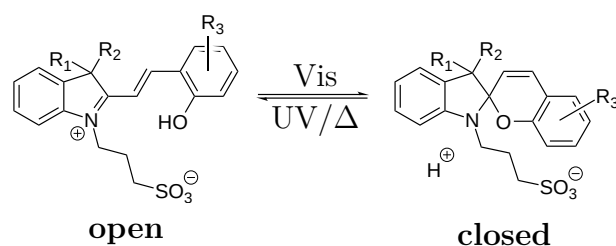


**Figure 1.6:** Merocyanine-type mPAHs

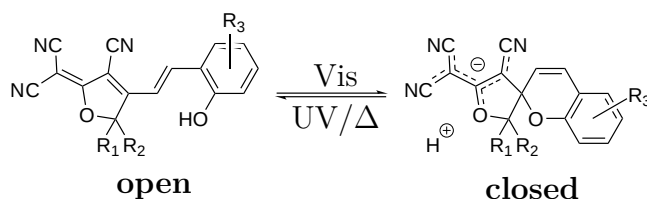


**Figure 1.7:** Tricyanofuran-type mPAHs

In stabilizing the open form, mPAHs avoid the need of UV light to drive the photoisomerization (closed to open), requiring visible light instead (open to closed). Aside from making mPAHs more practical for biological applications, the use of visible light alleviates photodegradation - one of the weak points of traditional spiro compounds. As mentioned in the previous section, the stabilization of the open form can be achieved on a normal spiropyran structure by attaching electron-withdrawing groups on the chromene moiety. This approach, however, is only partially successful in shifting the equilibrium towards the open form and tends to introduce low-lying triplet states in the photo-induced ring opening process.<sup>37 – 40</sup> Triplet excited states allow said compounds to interact with molecular oxygen upon excitation, which invigorates the photo-degradation quantum yield. As so, mPAHs are the best candidates for stabilizing the open form because they do so effectively and bypass the requirement of strongly electron-withdrawing groups and hence avoid introducing triplet states.

Another attractive feature of mPAHs is that they are inherently protonated. Upon ring closing, mPAHs release their phenol proton and acidify the environment. In returning to the open form, mPAHs recapture the proton from solution and increase the pH to its initial state. Since this process can be controlled via radiation with visible light, mPAHs allow for the remote modulation of pH. Traditionally, pH modulation with photochromic compounds has been accomplished with spiropyrans.<sup>41, 42</sup> The shortcoming of such systems is that they require prior acidification which is, once again, a harsh requirement for biological applications. So-called photoacid generators are also used to acidify the environment but, unlike spiro compounds, they are unable to recover the proton for further use.<sup>43 – 45</sup> Indeed, the only "reversible photoacid generator" that Martin et al. report on their review<sup>45</sup> are Liao's mPAHs,<sup>35</sup> which would not qualify as photoacid generators if one is to define them as compounds that degrade upon photoexcitation. An alternative way to modulate acidity is through aromatic alcohols, such as naphthols, which reversibly release their protons upon excitation. Nonetheless, unlike spiro compounds, they retain their ground state geometry for the most part. As so, excitation is not accompanied by a structural change that drastically modifies their absorbance profile.<sup>46, 47</sup>

Thus, mPAHs are the only reported compounds that reversibly modulate pH in tandem with a change in the absorbance profile and dipole moment, require visible light for photoisomerization, and circumvent the need of prior acidification. This ensemble of photochromic properties have led mPAHs to be used for pH/fluorescence modulation,<sup>17</sup> catalysis and hydrogel-volume control,<sup>36</sup> polymer functionalization<sup>36, 48, 49</sup> and cation detection.<sup>49, 50</sup> Liao gives a comprehensive list of the application of mPAHs.<sup>51</sup>

### 1.3 STUDYING mPAHS WITH ELECTRONIC STRUCTURE

The promise of mPAHs as molecular switches warrants the study of their structure and reactivity. Computational chemistry provides a series of powerful tools that can be used to that end. Electronic structure calculations could be used for fundamental inquiries on the thermodynamics of the mPAH forms (**open** vs. **closed**), the kinetics of the photoisomerization process, and the substituent effect thereon. Previously, electronic structure methods have been used to study the ring-opening process of other spiro compounds-primarily spiropyrans and spironaphthoxazines.<sup>52-57, 61</sup> Perhaps since most spiro compounds are thermodynamically stable in their closed form, the literature on the photoisomerization has a marked emphasis on the ring-opening reaction. Indeed, Minkin points out this disproportionality in his review.<sup>33</sup> More recently, some studies have focused on the ring-closing reactions, both thermally<sup>57</sup> and through the excited state<sup>74</sup>. Due to their advantages regarding application, it would be interesting to look into the isomerization processes in mPAHs and compare them to those of other spiro compounds.

## RESOLVING THE ISOMERIC IDENTITY OF TCF 1

Before any of the aforementioned studies can be performed on mPAHs, the identity of mPAHs in solution must be established. Four open and two closed conformations are possible. The two possible closed conformers are enantiomers because of the chiral spiro carbon. The four possible open conformers correspond to rotations about the  $\alpha$  and  $\gamma$  bonds. Only conformers of the trans configuration about the  $\beta$  bond are considered, since the cis configurations are unfavorable and are proposed to be found only as intermediates in the photoisomerization process, or under certain forcing conditions.<sup>52, 54, 56 – 58</sup> Theoretical and experimental studies on spironaphthoxazines and spiropheanthrooxazines establish TTC and CTC to be the preferred conformers on solution for these compounds.<sup>56 – 60</sup> For spiropyrans, the only study found to explicitly deal with the four open isomers also determined the TTC isomer to be the most stable.<sup>61</sup> In the case of spiropyrans, no experimental evidence was found as to whether only the TTC or multiple isomers coexist in solution. No studies on the two closed enantiomers for any spiro compound could be found either, but authors often refer to the symmetry of the planar open forms to attest to the existence of both closed enantiomers (e.g. since the open form has a plane of symmetry it can close on both directions to produce both enantiomers).

In any case, it can only be vaguely argued that the relative stability of open form isomers calculated for spiropyrans, or the proposed isomeric make up of



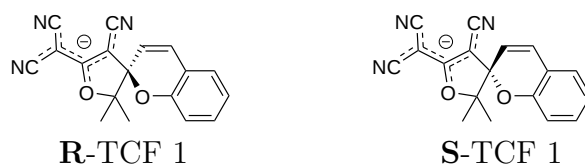


**Figure 2.1:** Closed enantiomers of TCF 1

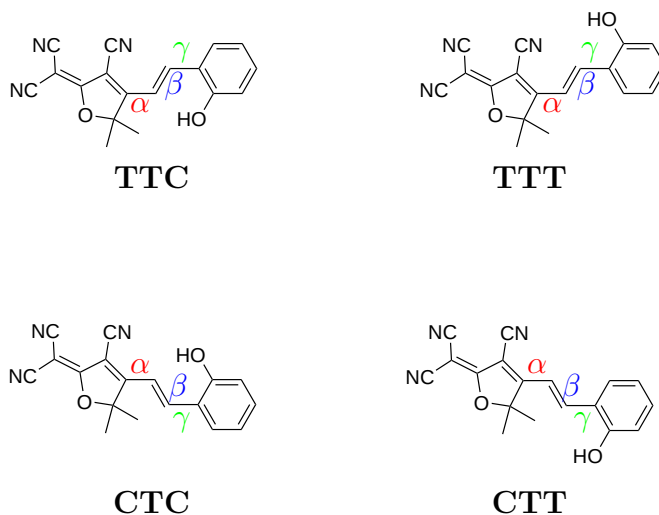


**Figure 2.2:** Open conformations of TCF 1

spironaphthoxazines and spirophenanthrooxazines applies to TCF mPAHs without further evidence. TCF mPAHs feature a completely different acceptor moiety and do not have restrictive nitrogen atoms bridging the acceptor and donor moieties, as is the case for spironaphthoxazines and spirophenanthrooxazines. As a result, it is plausible for TCF mPAHs to have different open-form isomers present in solution.

To find out which open form isomers for TCF 1 are present, a series of NMR experiments were performed. One-dimensional  $^1\text{H}$  and  $^{13}\text{C}$  NMR experiments, run overnight, provided chemical shifts for both of these nuclei and some  $J_{HH}$  values. HSQC and HMBC 2D NMR experiments were conducted to assign most of the chemical shifts to specific atoms in the molecule. Finally, an NOE experiment gave unambiguous evidence for the isomers present in solution by showing the

interactions of hydrogen nuclei close in space. The appendix at the end of this chapter contains all the raw experimental data for reference.

## 2.1 HETERONUCLEAR SINGLE QUANTUM CORRELATION NMR EXPERIMENT

A series of 2D NMR experiments were ran on TCF 1 in DMSO. The first one was a heteronuclear single quantum correlation (HSQC) experiment. This technique results in a 2D spectra, with a  $^1\text{H}$  NMR on one axis and a  $^{13}\text{C}$  NMR on the other one. Taking the  $^1\text{H}$  shieldings to correspond to the x-axis and the  $^{13}\text{C}$  shieldings to correspond to the y-axis, the interactions of a hydrogen with shielding  $x_1$  and a carbon with shielding  $y_1$  will show up at point  $(x_1, y_1)$ . The HSQC experiment is designed to exclusively capture the interactions between carbons and hydrogens that are one bond apart from each other.

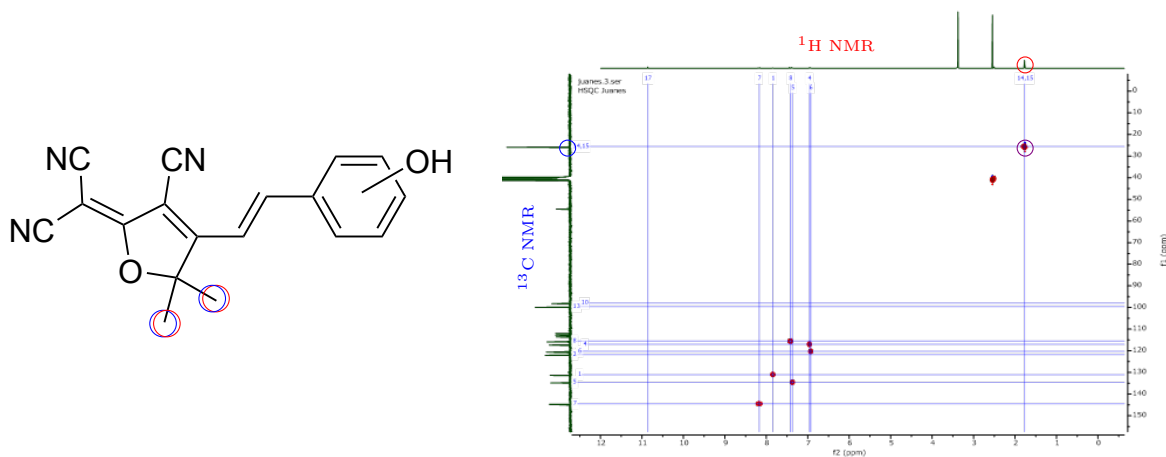


**Figure 2.3:** HSQC spectra for TCF 1

To illustrate, Figure 2.3 shows the HSQC spectra for TCF 1. The  $^1\text{H}$  signal circled in red unambiguously corresponds to the methyl hydrogens (circled in red

in the molecule), since they are the only hydrogens in the molecule capable of giving rise to signals in the aliphatic region. The 2D plane shows an interaction (circled in purple) with the carbon giving a signal at 25.52 ppm (circled in blue). Since the only carbons that are one bond away from the methyl hydrogens are the methyl carbons, it can be inferred that the signal at 25.52 ppm in the  $^{13}\text{C}$  NMR corresponds to the methyl carbons. This is, of course, a trivial example because the methyl carbons are the only carbons that can give rise to a signal in the aliphatic region. However, some non trivial information can be obtained from the rest of the interactions - all of which are listed in Table 2.3.

## 2.2 HETERONUCLEAR MULTIPLE BOND CORRELATION NMR EXPERIMENT

The heteronuclear multiple bond correlation (HMBC) experiment follows the same concept as the HSQC: Point  $(x_1, y_1)$  correspond to interactions between the hydrogen giving rise to the  $^1\text{H}$  shielding at  $x_1$  and the carbon giving rise to the  $^{13}\text{C}$  shielding at  $y_1$ . As opposed to the HSQC, however, the HMBC captures interactions of hydrogens and carbons that are exclusively two, three, and some times four bonds apart.

To illustrate, Figure 2.4 shows the HMBC spectra for TCF 1. The  $^1\text{H}$  signal circled in red corresponds to the methyl hydrogens (circled in red in the molecule) as established in the previous section. The 2D plane shows three interactions (circled in purple) with the carbons giving a signals at 25.1, 99.0 and 176.2 ppm (circled in blue). The signal at 25.52 was already accounted for - it corresponds to the methyl hydrogens interacting with the other methyl carbon (i. e. not the

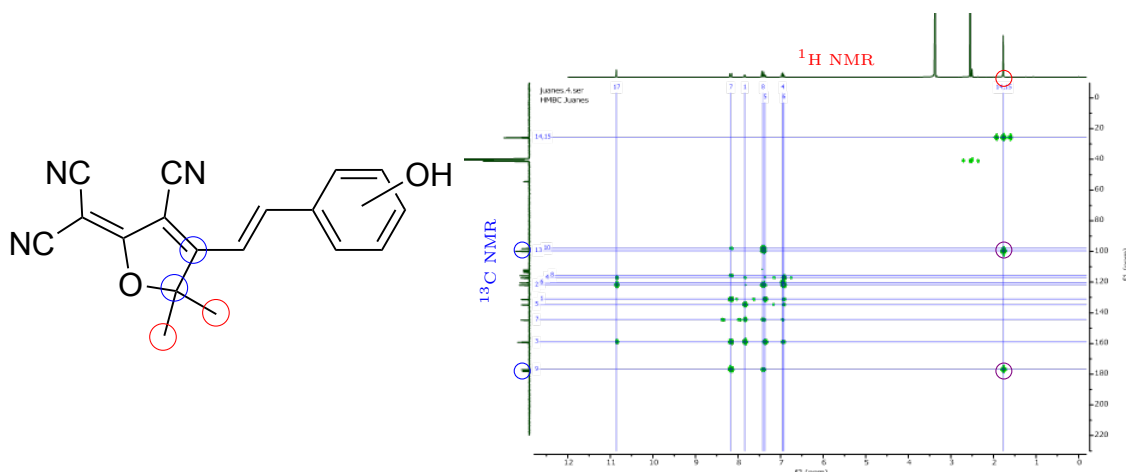


**Figure 2.4:** HMBC spectra for TCF 1

one they are directly bound to, since single-bond interactions don't show up in an HMBC). The other two carbons that are two and three bonds away from the methyl hydrogens are circled in blue in the molecule. It can be concluded that the two signals labeled in blue arise from the carbons also circled in blue.

The information in the HSQC and HMBC spectra allows to assign most signals in the 1D  $^1\text{H}$  and  $^{13}\text{C}$  NMR spectra. Only the shieldings for some carbons that are more than 4 bonds away from any hydrogen, such as the cyano carbons, cannot be determined unambiguously. Theoretical calculations (explained in the next chapter) were required to assign these. Figure 2.5 shows the carbon and hydrogen atoms of a TCF 1 molecule labeled with their associated chemical shieldings. Carbon shieldings are given in blue and hydrogen shieldings are given in red.

## 2.3 NUCLEAR OVERHAUSSER EFFECT NMR EXPERIMENT

The nuclear Overhauser effect (NOE) NMR experiment conducted for this project measures the dipole-dipole interactions between hydrogens in the molecule. This

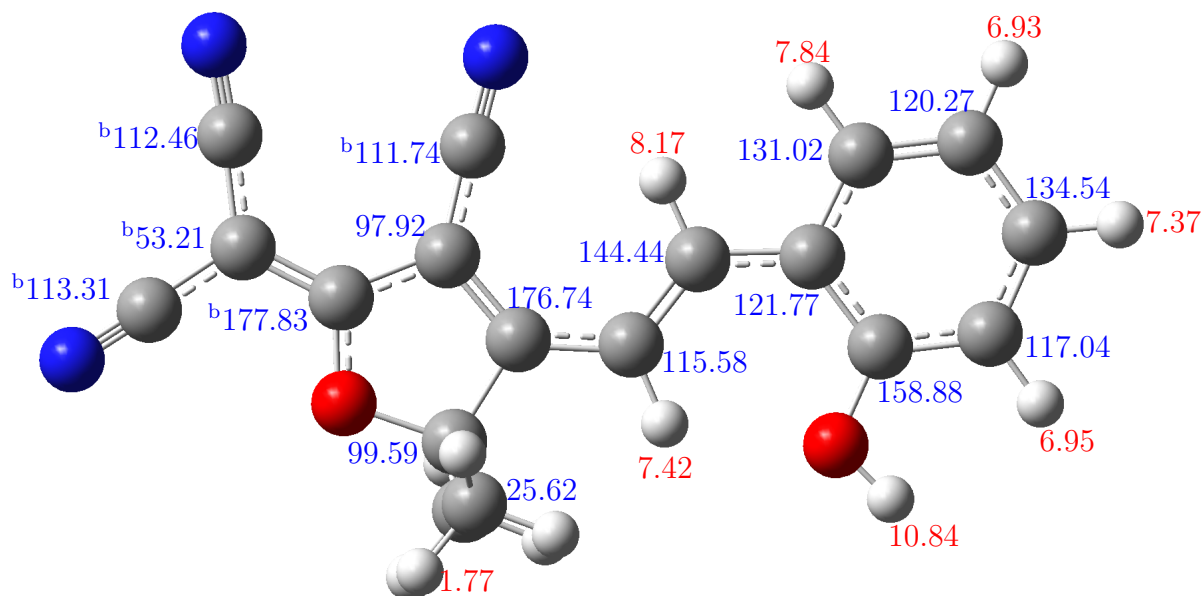


**Figure 2.5:** Chemical shieldings for TCF 1

<sup>a</sup> Absolute-reference calibrated. Disregarding conformation;

<sup>b</sup> Theoretical NMR calculations were required to assign these.

means that hydrogens that are close in space, but not necessarily in chemical bonding, will give a signal in the NOE 2D plane. Armed with the knowledge of every  $^1\text{H}$  (and  $^{13}\text{C}$ ) NMR shielding in the molecule, obtained from the HSQC and HMBC experiments, the NOE allows to determine which hydrogens are near to each other.

Three interactions of the vinyl hydrogens ( $^1\text{H}$  shieldings at 7.42 and 8.17, referred to as vinyl A and vinyl B from here on to make the distinction clear) were of particular interest in the case at hand:

- With the methyl hydrogens ( $^1\text{H}$  shieldings at 1.77 ppm)
- With the alcohol hydrogen ( $^1\text{H}$  shieldings at 10.86 ppm)
- With one of the aromatic hydrogens ( $^1\text{H}$  shielding at 7.84 ppm)

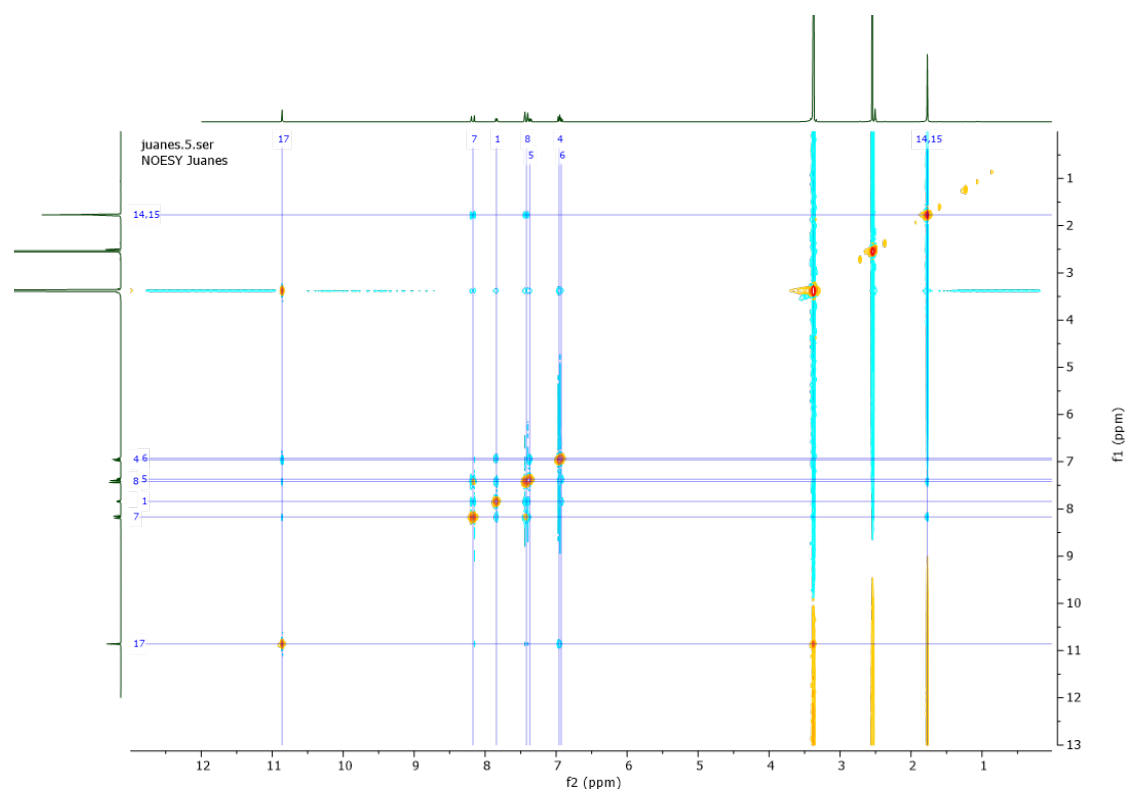


**Figure 2.6:** NOE spectra for TCF 1

Interactions of both vinyl A and vinyl B hydrogens with each of the three hydrogens just listed were found in the NOE. Since some of the signals are difficult to observe in the raw spectra (Figure 2.6), all the information is listed in Table 2.4.

The interaction of the methyl hydrogens with vinyl hydrogen B, labeled as a cyan curve in Figure 2.7, requires the presence of the CTC isomer, the CTT isomer, or both. The interaction of the aromatic hydrogen with vinyl hydrogen A, labeled as a green curve in Figure 2.7, requires the presence of the TTT isomer, the CTT isomer, or both. This same process can be repeated with every signal present. There are three ways to account for all interactions:

1. Only the TTC and CTT forms are present in solution

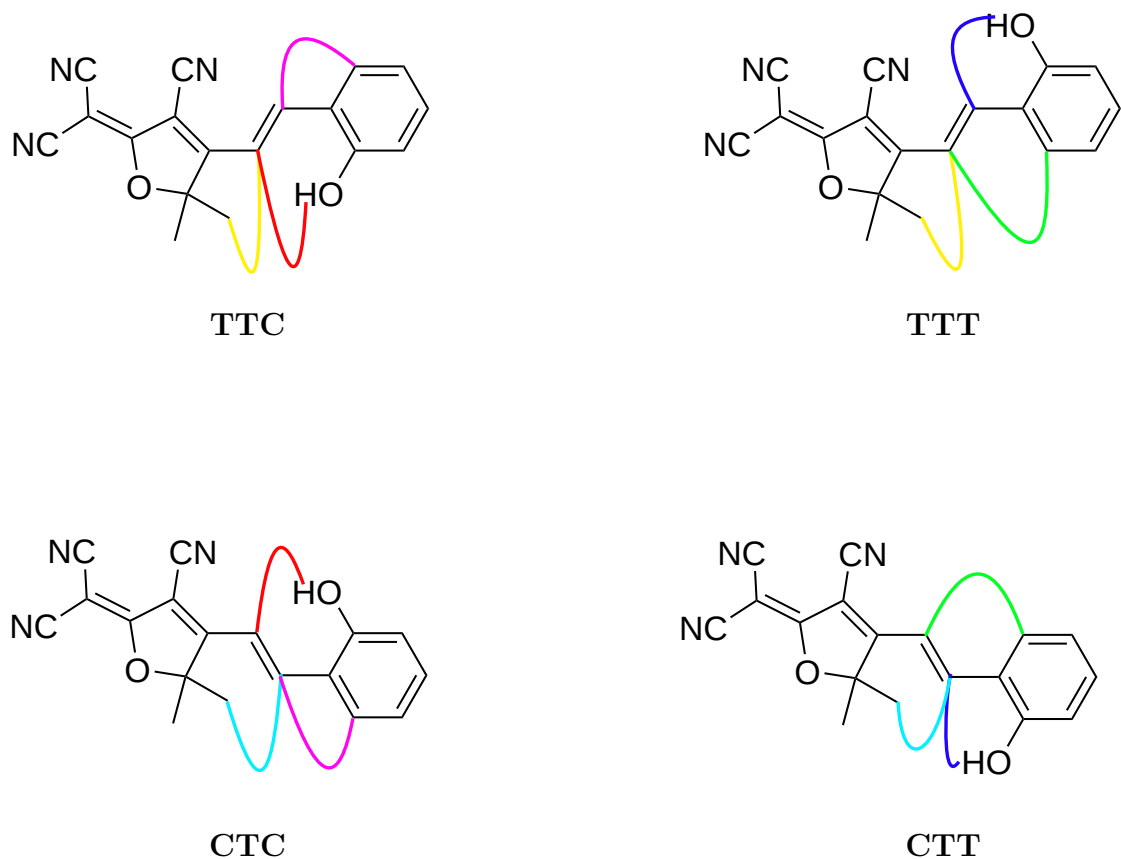


**Figure 2.7:** Relevant NOE interactions observed

2. Only the TTT and CTC forms are present in solution
3. All forms are present in solution

Case 3 seems the most plausible of all: There seems to be no reasons why two particular species are exclusively present in solution. The next chapter provides a more solid argument for case 3. These results are interesting because, as mentioned in the introduction to the chapter, previous studies on other spiro compounds have arrived at different conclusions. Experimentally, spironaphthoxazines<sup>58</sup> and spiropheanthrooxazines<sup>59</sup> were determined to exist only in the TTC and CTC conformations. However, the study by Lee et al.<sup>59</sup> was performed at 77 K which

raises the question as to whether the results hold at other temperatures. Additionally, they reach their conclusion under a dubious assumption (explained in the Discussion and Future Work chapter). The fact that one of the particular conformers might be more stable (as calculated for spiropyrans, for example) does not imply the lack of contributions to the population from the other conformers. Whether all isomers actually coexist in solution for spiropyrans, as is the case for TCF 1, remains to be established experimentally. In any case, the presence of several isomers has implications in the photoisomerization process: Not all open-form isomers may be able to access the closed form directly. This point will be elaborated on in the Discussion and Future Work chapter.

## 2.4 APPENDIX FOR CHAPTER 2

This section contains all the experimental NMR information including:

- 1D  $^1\text{H}$  NMR spectra
- 1D  $^{13}\text{C}$  NMR spectra
- HSQC NMR interactions
- HMBC NMR interactions
- NOE NMR interactions



**Table 2.1:** Information in  $^1\text{H}$  NMR spectra for TCF 1

Shielding (ppm)	Integration <sup>a</sup>	Multiplicity <sup>b</sup>	J-coupling <sup>c</sup> (Hz)
0.003 (TMS)	-	-	
1.768	6.06	s	-
2.500 (H <sub>2</sub> O)	-	-	
3.336 (DMSO)	-	-	
6.926	approx. 1	multiplet <sup>d</sup>	0.8
6.956	approx. 1	dd	0.8, 8.4
7.367	approx. 1	multiplet <sup>d</sup>	1.6
7.420	approx. 1	d	16.4
7.844	1.05	dd	1.4, 7.8
8.168	1.00	d	16.4
10.836	1.01	s	-

<sup>a</sup> The integration of overlapping peaks can only be approximated;<sup>b</sup> s = singlet, d = doublet, dd = doublet of doublets;<sup>c</sup> For the multiplets, only the smallest J-coupling could be obtained due to overlap with other peaks;<sup>d</sup> Possibly doublets of doublets of doublets (ddd).**Table 2.2:** Information in  $^{13}\text{C}$  NMR spectra for TCF 1

Shielding (ppm)
0.025 (TMS)
25.065
39.430 (DMSO)
53.653
97.379
99.041
111.181
111.903
112.754
115.020
116.483
119.707
121.216
130.493
133.978
143.886
158.327
176.184
177.277

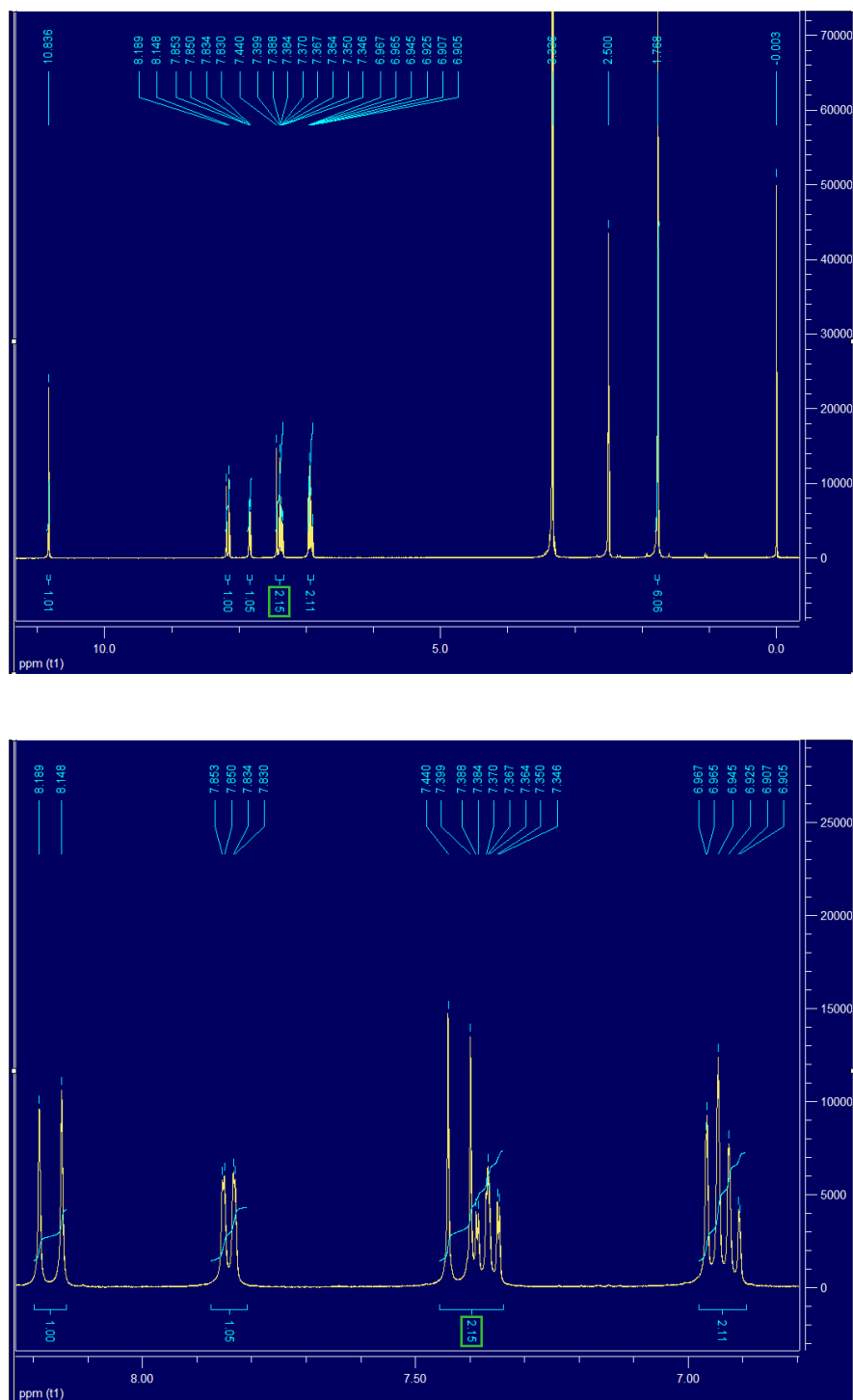


**Figure 2.8:** Full (above) and zoomed-in (below) 1D  $^1\text{H}$  NMR for TCF 1

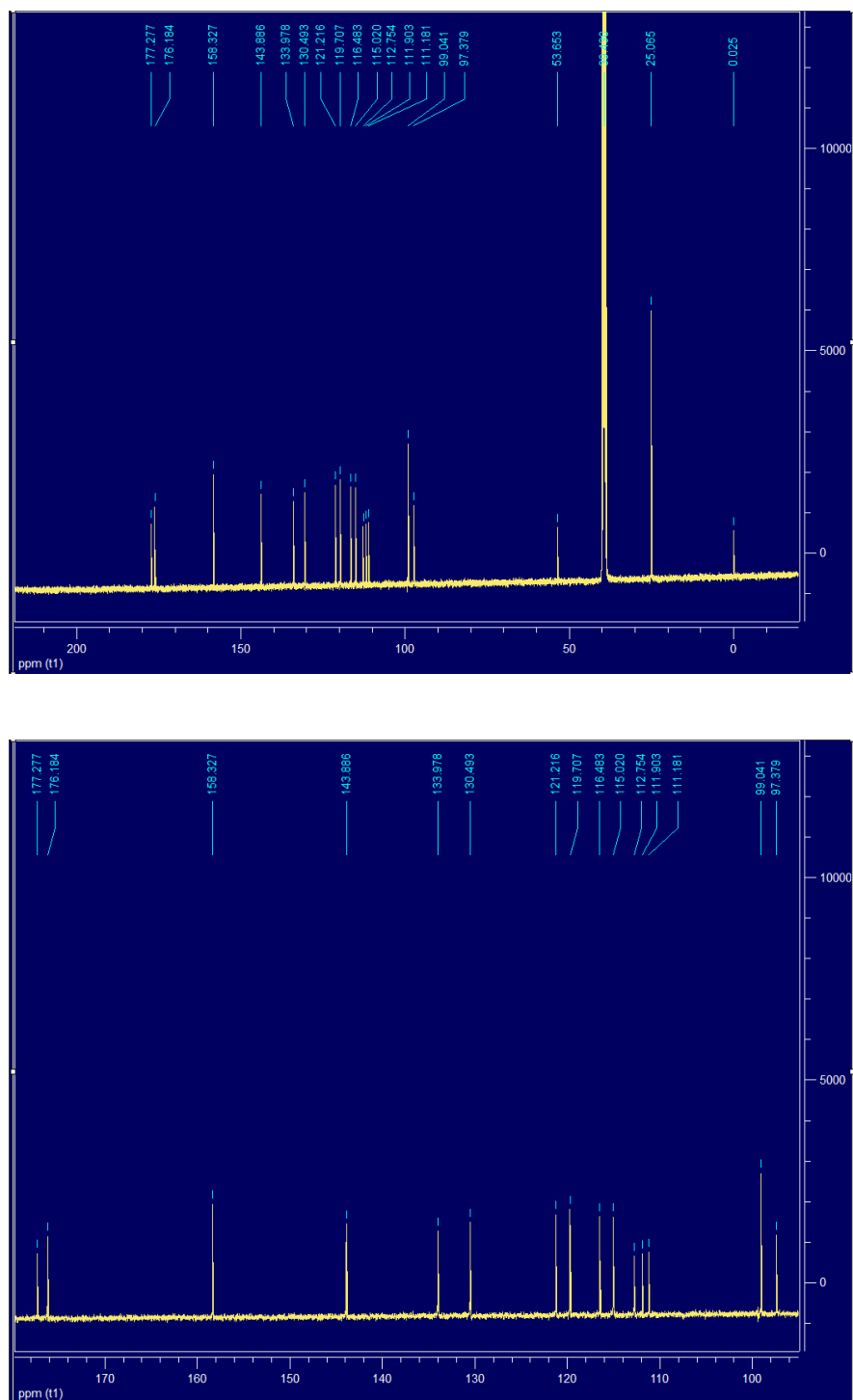


**Figure 2.9:** Full (above) and zoomed-in (below) 1D  $^{13}\text{C}$  NMR for TCF 1

**Table 2.3:** HSQC and HMBC interactions for TCF 1

	10.84	8.17	7.84	7.42	7.37	6.96	6.93	1.77
25.1								●●
53.7								
97.4		●		●				
99.0				●				●
111.2								
111.9								
112.8								
115.0		●		●				
116.5	●		●			●		
119.7							●	
121.2	●		●	●				
130.5		●	●		●		●	
134.0			●		●		●	
143.9		●	●	●		●		
158.3	●	●	●		●	●		
176.2		●		●				●
177.3								

<sup>a</sup> The vertical axis corresponds to the  $^{13}\text{C}$  NMR shieldings and the horizontal axis corresponds to the  $^1\text{H}$  NMR shieldings.

<sup>b</sup> HSQC and HMBC interactions are denoted with ● and ●, respectively.

**Table 2.4:** NOE interactions for TCF 1

	10.84	8.17	7.84	7.42	7.37	6.96	6.93	1.77
1.77		●		●				●
6.93			●		●		●	
6.96	●				●	●		
7.37					●	●	●	
7.42	●	●	●	●				●
7.84		●	●	●			●	
8.17	●	●	●	●				●
10.84	●	●		●		●		

<sup>a</sup> Both axes correspond to  $^1\text{H}$  NMR shieldings;

<sup>b</sup> NOE interactions are denoted with ●.

## ELECTRONIC STRUCTURE CALCULATIONS

The four open conformers and the two closed enantiomers were optimized to the B3LYP<sup>62,63</sup>/6-311++G(2d, p) and MP2<sup>64</sup>/6-311+G(d, p) levels of theory. The zero-point-energy (ZPE) corrections were made at the 6-311++G(2d, p) and 6-31G(d) basis sets for B3LYP and MP2, respectively. The polarizable continuum model<sup>65</sup> (PCM) was used to account implicitly for DMSO as the solvent.

These basis sets were the limits of our computational resources with the algorithms used for the calculations.

### 3.1 ENERGIES AND BOLTZMANN DISTRIBUTIONS

The four open forms, both in their protonated and deprotonated states, and the two closed enantiomers were modeled using the levels of theory mentioned above. Table 3.1 lists the ZPE-corrected energies of the optimized geometries of the open-protonated forms (denoted by their  $\alpha$ -,  $\beta$ -, and  $\gamma$ -bond conformations), the open-deprotonated forms (same notation, but labeled with<sup>-1</sup>), and the closed forms (R and S enantiomers). DMSO was used as the PCM. The corresponding Boltzmann distributions at room temperature were calculating according to

$$P_j = \frac{e^{-\beta E_j}}{\sum_i e^{-\beta E_i}} \quad (3.1)$$

**Table 3.1:** Normalized energies (kJ/mol) for TCF 1 isomers

Conformer <sup>a</sup>	B3LYP/6-311++G(2d, p)		MP2/6-311+G(d, p)	
	Energy	Distribution	Energy	Distribution
TTC	0.533	31.6%	0.000	30.2%
CTC	2.906	12.1%	0.324	26.5%
TTT	2.048	17.1%	1.853	14.3%
CTT	0.000	39.2%	0.094	29.0%
TTC <sup>-1</sup>	55.1	0%	-	-
CTC <sup>-1</sup>	58.7	0%	73.9	0%
TTT <sup>-1</sup>	57.7	0%	-	-
CTT <sup>-1</sup>	55.1	0%	74.7	0%
R <sup>-1</sup>	80.9	0%	26.9	0%
S <sup>-1</sup>	81.7	0%	27.5	0%

<sup>a</sup> The energy of a DMSO-solvated proton was added to the anionic species.

where  $E_j$  corresponds to the energy of the isomer in question,  $\beta$  to the thermodynamic beta at room temperature (298.25 K), and where the summation runs over all the the isomers. B3LYP and MP2 agree in the general description of the isomeric composition of the open-protonated form. Although differing in the fine details, both methods predict a substantial population of all the open-protonated isomers. This is in perfect agreement with the results obtained from the NMR experiments.

However, the methods are in complete disagreement in regards to the energy trends in the anionic species, namely, the open-deprotonated and closed forms. B3LYP predicts the open-deprotonated forms to be less stable than the closed form by a relatively large margin, whereas MP2 predicts the opposite. This discrepancy might be partially due in that the anionic species are often more difficult for traditional electronic structure methods to understand . This deserves a full-fledged study on its own right and will only be pointed out in this thesis.

In order to explore the viability of interconversion between the open protonated

forms, all the possible transition states between them were optimized using the Synchronous Transit-Guided Quasi-Newton (STQN) method. The eight possible transition states correspond to rotations, either clockwise or counterclockwise about the  $\alpha$  or  $\gamma$  bonds. Table 3.2 lists the B3LYP ZPE-corrected energies in DMSO as the PCM. The highest rotational barrier (39.020 kJ/mol) corresponds to the transition state in between the TTC and the CTC isomers, rotating clockwise. For comparison, the energies of rotation (in kJ/mol) for several common organic molecules are listed below:

- C-C bond in 1-chloroethanol:<sup>66</sup> 20.7
- (2, 3) C-C bond in n-butane:<sup>67</sup> 21.3
- (carbonyl) C-N bond in N, N-dimethylacetaamide:<sup>68</sup> 64.0 - 80.8 (depending on conditions)
- C-N bond in acetamide:<sup>69</sup> 72.4

All the rotational barriers for open-protonated TCF isomers fall in between the rotation of the C-C bond in n-butane, a full-fledged single-bond, and the rotation of the (carbonyl) C-N bond in N, N-dimethylformamide, which has a partial double-bond character due to resonance. As so, the open isomers are likely to interconvert between each other at a slightly slower rate than that of traditional single-bond alkyl chains. One could use the Eyring-Polanyi equation

$$k = \frac{\kappa k_B T}{h} e^{-\frac{\Delta G^\ddagger}{RT}} \quad (3.2)$$

to provide a definite rate constant but that requires knowledge of  $\kappa$ , the so-called

transmission coefficient. The best that the values calculated in this project can provide is the rate constant over  $\kappa$ . These values are listed in Table 3.2.

**Table 3.2:** Normalized energies (kJ/mol) for TCF 1 open-protonated forms and transition states, with the corresponding reaction rate constants.

Conformer	Energy	Reaction rate constant ( $\frac{1}{\kappa \text{ sec.}}$ ) <sup>c</sup>
TTC	0.533	-
CTC	2.906	-
TTT	2.048	-
CTT	0.000	-
TS <sub>TTC-TTT</sub> <sup>a</sup>	36.090	$3.628 * 10^6$
TS <sub>TTC-TTT</sub> <sup>b</sup>	37.810	$1.812 * 10^6$
TS <sub>TTC-CTC</sub> <sup>a</sup>	39.020	$1.112 * 10^6$
TS <sub>TTC-CTC</sub> <sup>b</sup>	38.777	$1.227 * 10^6$
TS <sub>CTT-CTC</sub> <sup>a</sup>	36.079	$2.939 * 10^6$
TS <sub>CTT-CTC</sub> <sup>b</sup>	36.294	$2.694 * 10^6$
TS <sub>CTT-TTT</sub> <sup>a</sup>	38.647	$1.043 * 10^6$
TS <sub>CTT-TTT</sub> <sup>b</sup>	37.313	$1.786 * 10^6$

<sup>a</sup> Rotating clockwise as seen from the phenol-end of the molecule;

<sup>b</sup> Rotating counter-clockwise as seen from the phenol-end of the molecule;

<sup>c</sup> The Gibbs free energy of activation  $\Delta G^\ddagger$  is calculated as the difference in energies between the transition state and the most stable of the two stable isomers in question

## 3.2 STRUCTURAL PARAMETERS

The structural parameters relevant to the interconversion of the different open TCF forms, namely the bond of the  $\alpha$ ,  $\beta$ , and  $\gamma$  bonds are listed in Table 3.3.

The bond lengths follow clear trends. B3LYP predicts the four TCF isomers to have longer  $\alpha$  and  $\gamma$  bonds, 1.422 and 1.442 Å on average, than  $\beta$  bonds, which average at 1.362 Å. For comparison, the C-C bonds in ethane and ethene are 1.54 and 1.34 Å, respectively. This suggests that  $\alpha$ ,  $\beta$ , and  $\gamma$  all have a partial double bond character, with the  $\beta$  bond more so than the other two. As the open-protonated forms interconvert between one another (i. e. at the transition



**Table 3.3:** Structural parameters for TCF 1 isomers

	B3LYP/6-311++G(2d, p)			MP2/6-311+G(d, p) <sup>a</sup>		
Conformer	$\alpha$	$\beta$	$\gamma$	$\alpha$	$\beta$	$\gamma$
TTC	1.423	1.363	1.442	1.442	1.364	1.455
CTC	1.422	1.362	1.442	1.438	1.364	1.455
TTT	1.421	1.362	1.442	1.443	1.360	1.458
CTT	1.420	1.360	1.443	1.438	1.360	1.458
<b>Average</b>	1.422	1.362	1.442	1.440	1.362	1.456
TTC <sup>-1</sup>	1.400	1.392	1.401	-	-	-
CTC <sup>-1</sup>	1.393	1.391	1.406	1.410	1.388	1.418
TTT <sup>-1</sup>	1.389	1.394	1.400	-	-	-
CTT <sup>-1</sup>	1.389	1.392	1.401	1.404	1.390	1.410
<b>Average</b>	1.393	1.392	1.402	1.407	1.389	1.414
TS <sup>a</sup> <sub>TTC-TTT</sub>	1.467	1.338	1.465	-	-	-
TS <sup>b</sup> <sub>TTC-TTT</sub>	1.467	1.338	1.464	-	-	-
TS <sup>a</sup> <sub>TTC-CTC</sub>	1.467	1.341	1.461	-	-	-
TS <sup>b</sup> <sub>TTC-CTC</sub>	1.467	1.341	1.462	-	-	-
TS <sup>a</sup> <sub>CTT-CTC</sub>	1.438	1.343	1.483	-	-	-
TS <sup>b</sup> <sub>CTT-CTC</sub>	1.438	1.343	1.483	-	-	-
TS <sup>a</sup> <sub>CTT-TTT</sub>	1.441	1.343	1.483	-	-	-
TS <sup>b</sup> <sub>CTT-TTT</sub>	1.441	1.343	1.483	-	-	-
<b>Average</b>	1.453	1.341	1.473	-	-	-

<sup>a</sup> The transition states were not calculated with the MP2 method. The TTC<sup>-</sup> and TTT<sup>-</sup> forms failed to converge despite repeated efforts.

state connecting two open-protonated forms), the  $\alpha$  and  $\gamma$  bonds elongate while the  $\beta$  bond contracts. This correlates well with the results obtained for the energies of rotation about the  $\alpha$  and  $\gamma$  bonds - they are comparable to those of a single bond with partial double bond character.

In the deprotonated states, the  $\alpha$  and  $\gamma$  bonds contract while the  $\beta$  bond elongates. A longer, weaker  $\beta$  bond due to deprotonation is more amenable to rotation. Rotation about the  $\beta$  bond, which has not been considered in this project, leads to the "cisoid" intermediates (about that bond) proposed by some authors to partake in the open-closed isomerization of similar spiro compounds.<sup>52, 54, 56</sup> It

is important to point out, however, that despite the slight elongation that occurs on the  $\beta$  bond upon deprotonation, it's length still falls closer to that of a double bond than to that of a single bond. This suggests that rotation about the  $\beta$  bond in the ground state surface, as is shown by Kohl-Landraf et al. for their water-soluble spiropyran,<sup>71</sup> would require a TCF 1 to be in a very hot vibrational state. Isomerization in the excited state surface would seem more plausible, as Sanchez-Lozano et al. consider in their study.<sup>74</sup> Worthy of mention, TCF 1 is able to overcome the thermal barrier for isomerization upon addition of base. The explanation as to how this happens is the subject of future studies in the Torres lab - perhaps a better treatment of the anionic species and explicitly modeling the transition state (as opposed to qualitatively relying on the length of the  $\beta$  bond) will result in a plausible thermal ring-closing pathway.

### 3.3 CHEMICAL SHIELDINGS

Comparing the chemical shieldings that the theoretical methods predict against their experimental values provides a way to gauge the accuracy of the predicted energies and structural parameters. The chemical shieldings using both B3LYP and MP2 were calculated from the corresponding optimized geometries. Figure 3.1 shows a labeling scheme for the hydrogens and carbons in the molecule. The theoretical values for every isomer were weighed by their corresponding Boltzmann distribution and added together. These Boltzmann-averaged theoretical shieldings were then compared against their experimental values using the normalized root-

mean-squared-deviation (NRMSD) statistic

$$NRMSD = \frac{100\%}{\sigma_{exp.}^{max.} - \sigma_{exp.}^{min.}} \sqrt{\frac{\sum_i^T (\sigma_{exp.} - \sigma_{theo.})^2}{T}} \quad (3.3)$$

where the exp. and theo. subscripts denote experimental and the theoretical chemical shifts, respectively, the min. and max. superscript denote their maximum values in the set being considered, and T corresponds to the total number of atoms being considered (17 for carbon, 8 for hydrogen), and the summation runs over all the atoms as well.

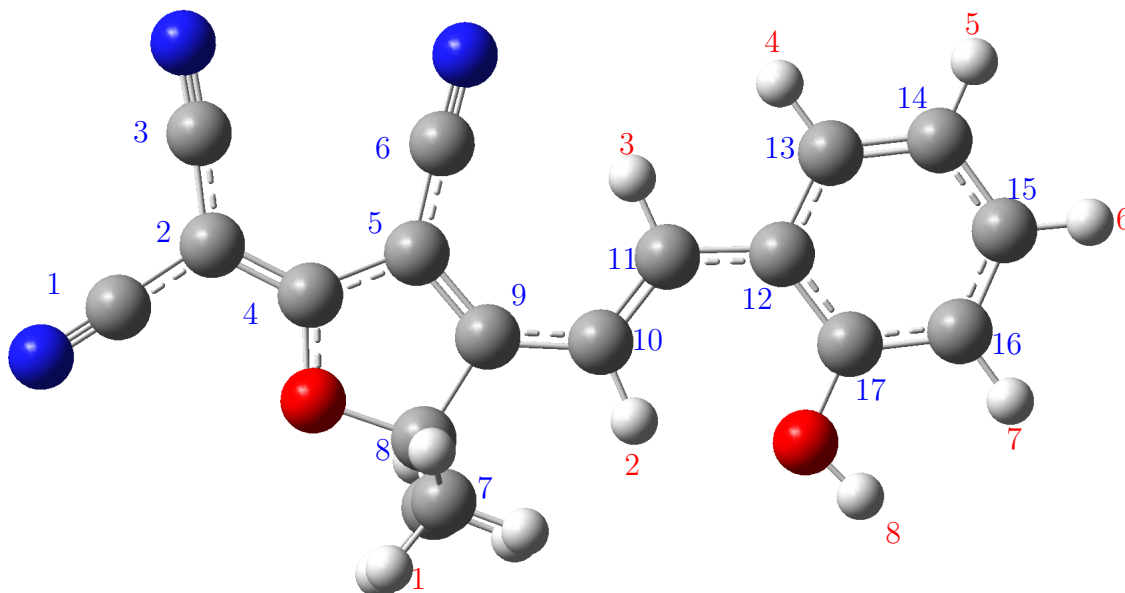


**Figure 3.1:** Labeling scheme for carbons and hydrogen in TCF 1

Table 3.4 shows the chemical shieldings for TCF 1 as calculated at the B3LYP/6-311++G(2d, p) level of theory. The B3LYP results are in relatively good agreement with the experiments, with a NRMSD of 4.67% for carbon atoms and of 3.82% for hydrogens. Note that the phenol hydrogen throws off the NRMSD if included in

the calculation of that statistic because the theoretical value differs by more than 5 ppm in this case. This is because the phenol hydrogen hydrogen bonds with the DMSO molecules in the solvent. The interaction can actually be seen in the NOE spectra in Figure 2.6 at (10.84, 3.33). So, the chemical shift for this hydrogen, as calculated from electronic structure is expected to be vastly different from its experimental value.

**Table 3.4:** Theoretical vs. experimental chemical shieldings for TCF 1 B3LYP/6-311++G(2d, p), single molecule.

<sup>13</sup> C shieldings						
Atom	TTT	TTC	CTC	CTT	Boltzmann avg.	Experimental <sup>a</sup>
1	120.83	120.81	120.53	120.55	120.68	112.73
2	53.20	53.20	53.73	58.80	55.46	53.63
3	120.01	120.01	119.99	119.98	120.00	111.88
4	187.28	187.38	189.39	187.86	187.80	177.25
5	94.34	93.93	100.78	100.32	97.33	97.35
6	119.72	119.78	117.64	117.58	118.65	111.16
7	25.24	25.50	27.23	27.47	26.44	25.04
8	106.43	106.60	105.56	105.78	106.12	99.02
9	186.49	187.77	186.06	186.13	186.70	176.16
10	115.55	121.45	122.79	116.86	118.80	114.80
11	151.78	158.45	158.07	151.16	154.41	143.86
12	125.68	126.29	125.97	125.39	125.79	121.19
13	132.42	143.71	143.60	132.36	137.32	130.47
14	125.79	125.66	125.59	125.81	125.73	119.68
15	143.35	142.06	141.67	143.03	142.61	133.95
16	120.20	120.49	120.56	120.02	120.26	116.46
17	166.30	167.18	166.73	165.69	166.39	158.02
<b>NRMSD</b>						<b>4.67%</b>

<sup>1</sup> H shieldings						
Atom	TTT	TTC	CTC	CTT	Boltzmann avg.	Experimental <sup>a</sup>
1	1.59	1.58	1.77	1.77	1.68	1.76
2	7.09	7.63	8.14	7.59	7.58	7.42
3	9.57	9.09	7.85	8.53	8.80	8.16
4	8.25	7.80	7.79	8.26	8.06	7.84
5	7.28	7.30	7.31	7.29	7.29	6.92
6	7.80	7.80	7.75	7.79	7.79	7.36
7	7.07	7.12	7.14	7.09	7.10	6.95
8	5.31	5.78	5.80	5.24	5.24	10.83
<b>NRMSD</b>	(including outlier) <sup>b</sup>					<b>21.1%</b>
<b>NRMSD</b>	(excluding outlier)					<b>3.82%</b>

<sup>a</sup> Calibrated by setting the TMS signal at 0 for comparison with theoretical spectra (those are calibrated like that as well);

<sup>b</sup> The outlier corresponds to the hydroxy hydrogen (labeled as hydrogen 8).

Modeling the TCF 1 isomers hydrogen-bonding to an explicit DMSO molecule improves the result on this hydrogen. The same procedure carried out up to this point was performed for the open- protonated TCF isomers hydrogen-bonding with an explicit DMSO molecule: The four isomers were optimized to B3LYP/6-311++G(2d, p); the Boltzmann populations and the weighed theoretical chemical shieldings were calculated, and the RMSD statistic was obtained by comparing to the experimental values. Indeed, the theoretical vs. experimental deviation for the phenol hydrogen improved dramatically. The results are shown in Table 3.5.

MP2 was also tested for completion. The shieldings were calculated at the 6-31+G(d, p) basis set, due to computational constrains (note: the shieldings were calculated from the geometries at that level). The NRMSD's are remarkably close to the B3LYP/6311++G(2d, p) accuracy, given the small basis set for this calculation.

In gauging the accuracy of the predictions, three things must be pointed out. The first is that, since the theoretical chemical shifts were calibrated to calculated chemical shifts for TMS, which carry an inherent error, the true accuracy of the predictions can only be better than the one reported here. The second is that the calculation of chemical shifts requires three separate processess: the optimization of the molecule's geometry to its lowest energy, the calculation of an energy, and the calculation of the chemical shieldings. That is to say, an error in any one of those processes (say, a calculated geometry that is slightly distorted from its true conformation, or the unavoidable deviation from the true energy) affects the resulting chemical shifts. So, the NRMSD reported here include any errors also coming from the geometry optimizations and the accuracy of the energies calculated. Unless these errors fortuitously cancel each other, the component of the NRMSD

that corresponds to deviations in the energies (the quantity that we are interested on, in the end) are smaller than the ones reported here. The third is that there is not a standard way to define an acceptable NRMSD; unlike with the standard deviation statistic, a confidence interval cannot be constructed. The NRMSD values reported here roughly mean that, for example, given any random carbon in the TCF 1 molecule, the B3LYP/6311++(2d, p) method is able to predict the chemical shift of any random carbon in the TCF 1 molecule to within  $\pm 4.67\%$  (in the scale of 25.04 - 177.25 ppm).

The interpretation of these numbers are then, to some extent, dependent on the reader. Nonetheless, they are clearly not outrageous. In fact, it seems almost remarkable that the methodologies used, especially B3LYP, are able to predict the chemical shifts of the open-protonated chemical shifts to such extent, given the need for reliable geometries and energies to calculate these. The fact that these calculations can predict chemical shifts to a reasonable extent adds confidence to the energies, Boltzmann distributions, and structural parameters obtained for said forms.

The same cannot be said for the open-deprotonated and the closed forms since no experimental data is available to compare. Additionally, the fact that the B3LYP and the MP2 results disagree in regards to the relative energies between the deprotonated species (i.e. the closed form and the open-deprotonated forms) forms is an indication that they require special attention when modeling with electronic structure methods.

**Table 3.5:** Theoretical vs. experimental chemical shieldings for TCF 1  
B3LYP/6-311++G(2d, p), hydrogen-bonding with an explicit DMSO molecule.

<sup>13</sup> C shieldings						
Atom	TTT	TTC	CTC	CTT	Boltzmann avg.	Experimental <sup>a</sup>
1	121.18	121.14	120.88	120.72	120.84	112.73
2	52.16	52.21	52.76	52.21	52.30	53.63
3	120.36	120.34	120.33	120.38	120.37	111.88
4	187.33	187.41	186.08	186.58	186.65	177.25
5	92.72	92.42	99.13	98.57	97.42	97.35
6	120.20	120.23	118.05	118.39	118.71	111.16
7	25.39	25.66	27.30	27.14	27.66	25.04
8	106.05	106.23	105.29	105.29	106.18	99.02
9	186.21	187.68	189.33	188.01	187.97	176.16
10	113.98	120.00	121.33	115.36	116.54	114.80
11	153.21	159.66	159.23	152.55	154.31	143.86
12	125.98	126.58	126.24	125.52	125.78	121.19
13	132.27	143.55	143.43	132.13	134.94	130.47
14	123.62	123.34	123.30	123.70	123.59	119.68
15	143.76	142.35	141.86	143.57	143.21	133.95
16	120.52	120.52	120.56	120.45	120.48	116.46
17	170.26	171.18	170.78	169.71	170.08	158.02
<b>NRMSD</b>						<b>4.76%</b>

<sup>1</sup> H shieldings						
Atom	TTT	TTC	CTC	CTT	Boltzmann avg.	Experimental <sup>a</sup>
1	1.58	1.57	1.76	1.76	1.72	1.76
2	6.96	7.76	8.28	7.47	7.56	7.42
3	9.64	9.09	7.85	8.62	8.62	8.16
4	8.15	7.70	7.65	8.15	8.03	7.84
5	7.10	7.12	7.13	7.11	7.11	6.92
6	7.73	7.73	7.72	7.70	7.71	7.36
7	7.28	7.34	7.39	7.26	7.29	6.95
8	12.43	12.91	13.00	12.35	12.51	10.83
<b>NRMSD<sup>b</sup></b>	(including outlier)					<b>7.21%</b>
<b>NRMSD</b>	(excluding outlier)					<b>3.18%</b>

<sup>a</sup> Calibrated by setting the TMS signal at 0 for comparison with theoretical spectra (those are calibrated like that as well);

<sup>b</sup> The outlier corresponds to the hydroxy hydrogen (labeled as hydrogen 8).



**Table 3.6:** Theoretical vs. experimental chemical shieldings for TCF 1  
MP2/6-31+G(d, p), single molecule.

<sup>13</sup> C shieldings						
Atom	TTT	TTC	CTC	CTT	Boltzmann avg.	Experimental <sup>a</sup>
1	108.40	108.44	108.47	108.36	108.42	112.73
2	50.12	49.91	49.94	50.44	50.44	53.63
3	109.63	109.70	109.43	109.30	109.50	111.88
4	161.71	161.80	160.86	160.84	161.26	177.25
5	90.50	90.24	95.50	95.92	93.32	97.35
6	111.25	111.12	108.85	108.72	109.84	111.16
7	19.79	19.87	21.96	21.98	21.02	25.05
8	93.30	93.10	92.40	92.72	92.83	99.02
9	157.70	160.77	157.81	156.31	158.25	176.16
10	106.82	110.72	112.37	108.68	110.01	114.80
11	125.82	128.32	128.68	124.89	126.96	143.86
12	114.45	113.19	113.42	114.77	113.89	121.19
13	110.26	117.92	117.81	110.30	114.58	130.47
14	111.63	111.77	112.02	111.71	111.80	119.68
15	115.80	115.22	115.15	115.88	115.48	133.95
16	105.79	106.62	106.93	105.68	106.31	116.46
17	141.56	142.96	142.82	141.30	142.24	158.86
<b>NRMSD</b>						<b>7.20%</b>

<sup>1</sup> H shieldings						
Atom	TTT	TTC	CTC	CTT	Boltzmann avg.	Experimental <sup>a</sup>
1	2.79	2.46	2.67	2.67	2.62	1.76
2	7.99	8.82	9.43	8.48	8.76	7.42
3	9.80	8.90	8.24	8.96	8.87	8.16
4	8.79	8.50	8.49	8.80	8.63	7.84
5	8.40	8.40	8.39	8.41	8.40	6.92
6	8.49	8.46	8.45	8.48	8.47	7.36
7	8.23	8.25	8.26	8.21	8.24	6.95
8	6.16	6.63	6.67	6.12	6.43	10.83
<b>NRMSD<sup>b</sup></b>	(including outlier)					<b>20.7%</b>
<b>NRMSD</b>	(excluding outlier)					<b>12.3%</b>

<sup>a</sup> Calibrated by setting the TMS signal at 0 for comparison with theoretical spectra (those are calibrated like that as well);

<sup>b</sup> The outlier corresponds to the hydroxy hydrogen (labeled as hydrogen 8).

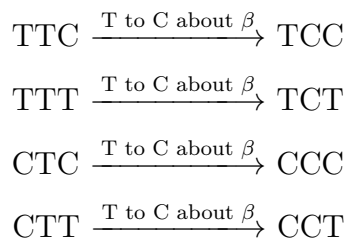
## DISCUSSION AND FUTURE WORK

This thesis concerned itself with answering a straightforward question: What are the protonated open-form isomers present in solutions for TCF mPAHs? The NOE experiments, armed with the knowledge of every chemical shielding provided by the HSQC and HMBC experiments, strongly suggested the presence of the four protonated open-form isomers corresponding to the XTY conformations about the  $\alpha$ ,  $\beta$ , and  $\gamma$  bonds (where X and Y can be either cis (C) or trans (T)). The Boltzmann populations, as calculated by the theoretical models used, provide further evidence that indeed, the four isomers are present. Furthermore, the calculated rotational barriers suggest a considerable degree of interconversion between the four isomers. To indirectly gauge the validity of the information obtained through the theoretical calculations, the methods used were employed to calculate theoretical chemical shieldings to compare against experimental values. The agreement between the two validates the information obtained through the theoretical calculations.

The unambiguous presence of the four open-protonated isomers with a trans conformation about the  $\beta$  bond in TCF mPAHs differs from the conclusions reached by some authors regarding similar compounds. For example, Nakamura et al. found only the analogous TTC isomer in spironaphthoxazines to be present in solution based on NOE NMR experiments.<sup>58</sup> Lee et al. claim only the TTC and CTC isomers to be present for spirophenanthrooxazines based on the fact that two signals,

at 172.6 and 178 ppm, are observed on the  $^{13}\text{C}$  NMR in the region corresponding to carbonyl carbons (170 - 180 ppm).<sup>59</sup> However, the present study found the signal for the highly de-shielded spiro carbon in TCF mPAHs to lie at 176.7 ppm, and it would be reasonable to contemplate the possibility of one of the signals reported by Lee et al. arising from the spiro carbon in the compound they studied, instead of a carbonyl carbon as they claim. If that were the case, then the remaining signal that they attributed to a single open form isomer might actually be a weighed average of more than one isomer, as is the case here.

Perhaps the most relevant consequence of the fact that all of the four open-protonated isomers are present is the implications this has in the isomerization processes. As mentioned before, the most plausible interconversion pathway connecting the open and closed forms of spiro compounds is proposed to proceed through a cisoid intermediate about the  $\beta$  bond.<sup>52, 54, 56</sup> Allowing only for one bond rotation at the time, every one of the four open-protonated isomers considered in this study can only access one cisoid intermediate. Figure 4.1 - 4.4 shows the optimized structures of the four cisoid intermediates at the B3LYP/6-311++G(2d,p) level of theory with DMSO as the PCM. For clarity, the two carbons that make up the  $\beta$  bond are highlighted in cyan and the methyl groups are omitted.



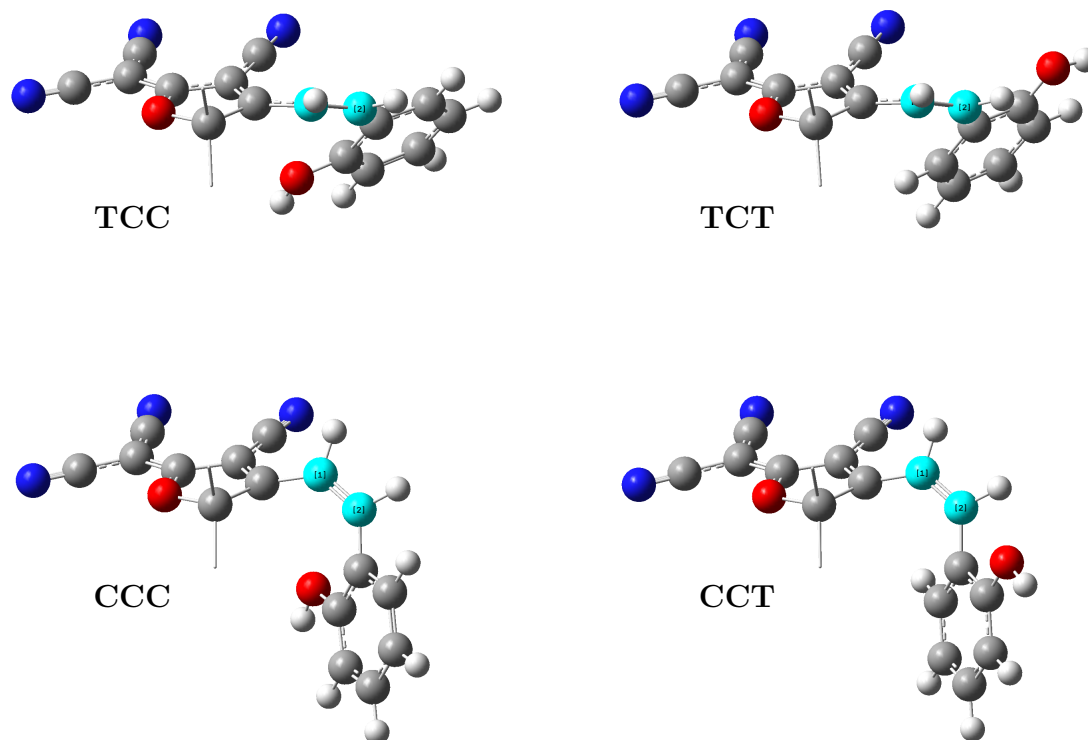
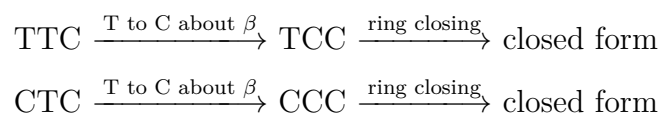
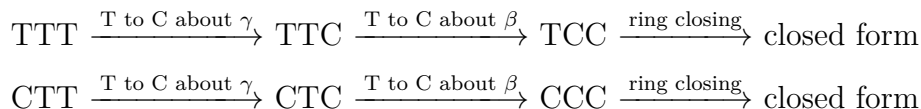


**Figure 4.1:** Cisoid intermediates for TCF 1

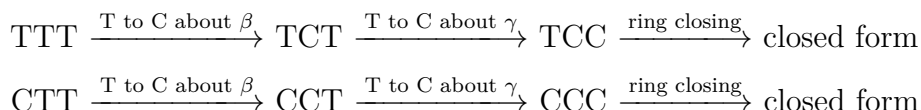
Out of the four, only the TCC and CCC cisoid intermediates can be conceived to lead to the closed form via a single transition state since the oxygen is pointing in the right direction for a nucleophilic attack at the spiro carbon. For the TCT and CCT isomers, the oxygen is pointing in the other direction. Therefore, the TTC and CTC isomers would only require two steps to reach the closed form:



The TTT and CTT forms would require at least three steps to reach the closed form:



or



Other exotic pathways connecting the stable open form isomers and the closed forms are sure to exist but it would be no surprise to find them to require great amounts of energy. For example, Horii et al. found an inversion pathway that connects the CTT and CCC isomers in spironaphthoxazines, but these compounds contain a nitrogen atom amenable to such a motion in the double bond connecting the donor and acceptor moieties.<sup>56</sup> A number of theoretical<sup>52, 53, 55</sup>, experimental<sup>70</sup>, and mixed theoretical/experimental<sup>61</sup> studies have concerned themselves with the closed to open reaction in spiro compounds through the excited state surface. A few other studies have either explored or exclusively focused the ground state surface and/or the open to closed process in different spiro compounds.<sup>56, 57, 71 – 74</sup>

It would be interesting to understand the excited-state and thermal processes between the open and closed forms in TCF mPAHs and compare them to those of other other spiro compounds. To that end, and based on the insight given by this work, the Torres group is currently studying the possible intermediates in the thermal isomerization process and the corresponding transition states connecting them, with hopes of studying the excited state surface at some point. Dr. Stéphane Aloïse, our colleague at l’Université de Lille 1, is finding (ultra-fast) spectroscopic

evidence of the species present in the photoisomerization and their lifetimes. A powerful experimental study, in tandem with comprehensive theoretical corroboration, promises to shed light into the nature of TCF mPAHs and improve our capacity to design photochromic molecular switches.

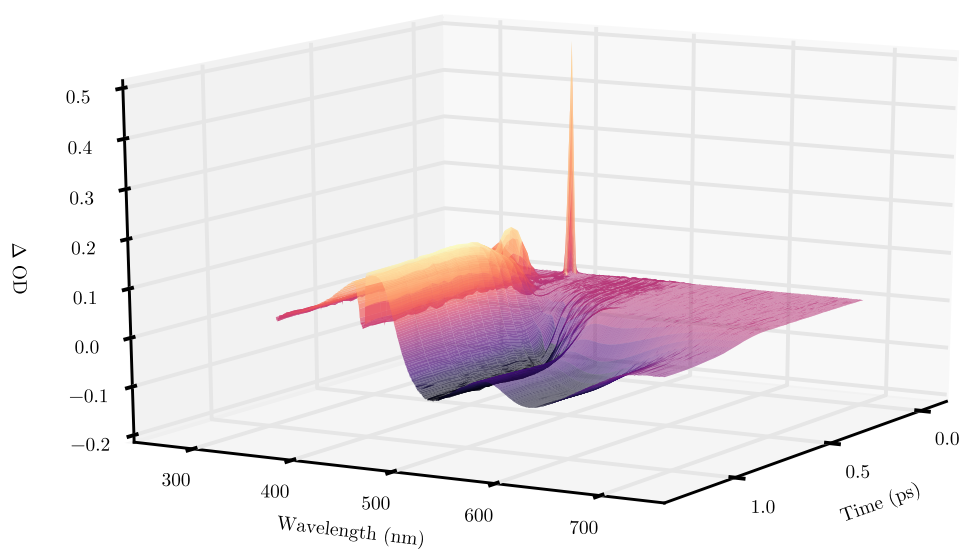


**Figure 4.2:** Transient absorbance spectra for TCF 1

## REFERENCES

1. Crano, J. C.; Guglielmetti, R. J. *Organic Photochromic and Thermochromic Compounds*, in Topics in Applied Chemistry; Springer: New York, NY, **2002**; p. 2.
2. Fisher, G.; Muszkat, K. A.; Fisher, E. *J. Chem. Soc. B.* **1968**, 0, 1156.
3. Buckles, R. E.; Wheeler, N. G. *Org. Synth.* **1953**, 33, 88.
4. Shriner, R. L.; Berger, A. *Org. Synth.* **1943**, 23, 86.
5. Cembran, A.; Bernardi, F.; Garavelli, M.; Gagliardi, L.; Orlandi, G. *J. Am. Chem. Soc.* **2004**, 126, 3234.
6. Brittain, W. J.; Rastagi, S. K.; Rogers, R. A.; Rinaldi, P. *J. Phys. Org. Chem.* **2018**, 31:e3847.
7. Yin, T. Zhao, Z.; Hong, Z. *Org. Elect.* **2018**, 52, 61.
8. Diau, E. W. *J. Phys. Chem. A.* **2004**, 108, 950.
9. Ishikawa, T.; Nuro, T. *J. Chem. Phys.* **2001**, 115, 7503.
10. Kathan, M.; Hecht, S. *Chem. Soc. Rev* **2017**, 46, 5536.

11. Shiroshi, Y.; Nakamura, M.; Hayashi, N.; Hirai, T. *Anal. Chem.* **2016**, 88, 6805.
12. Vales, T. P.; Badon, I. W. T.; Kim, H. *Macromol. Res.* **2018**, 26, 950.
13. Chung, D. J.; Ito, Y.; Imanishi, Y. *J. Appl. Pol. Sci.* **1994**, 51, 2027.
14. Bardavid, Y.; Goykhman, I.; Nozaki, D.; Cuniberti, G.; Yitzchoik, J. *J. Phys. Chem. C* **2011**, 151, 3123.
15. Connal, L. A.; Franks, G. V.; Qiuo, G. G. *Langmuir*. **2010**, 26, 10397.
16. Yu, Q.; Su, X.; Zhang, T.; Zhang, Y.; Li, M.; Liu, Y.; Zhong, S. X. *J. Mater. Chem. C* **2018**, 6, 2113.
17. Patel, P. K.; Arias, J. E.; Gongora, R. S.; Hernandez, F. E.; Moncomble, A.; Aloïse, S.; Chumbimuni-Torres, K. Y. *Phys. Chem. Chem. Phys.* **2018**, 20, 26804.
18. Fu, Y.; Han, H.; Zhang, J.; He, X.; Feringa, B. L.; Tian, H. *J. Am. Chem. Soc.* **2018**, 140, 8671.
19. Zhang, J.; Fu, Y.; Han, H.; Zang, Y.; Li, J.; He, X.; Feringa, B. L.; Tian, H. *Nat. Comm.* **2017**, 8, 1.
20. Yuan, W.; Gao, X.; Pei, E.; Li, Z. *Polym. Chem.* **2018**, 9, 3651.
21. Cho, M.; Kim, J.; Choi, H. J.; Choi, S. *Smart Mater. Struct.* **2017**, 26, 054007/1.
22. Ji, J.; Li, X.; Wu, T.; Feng, F. *Chem. Sci.* **2018**, 9, 3651.



23. Tyler, N. W. Jr.; Becker, R. S. *J. Am. Chem. Soc.* **1970**, 92, 1289.
24. Guglielmetti, R. J. *Photochromism: Molecules and Systems*, in Organic Chemistry; Durr, H., Bouas-Laurent, H., Eds.; Elsevier: Amsterdam, **1990**; pp 314 - 466 and 855 - 878.
25. Chu, N. Y. C. *Photochromism: Molecules and Systems*, in Organic Chemistry; Durr, H., Bouas-Laurent, H., Eds.; Elsevier: Amsterdam, **1990**; pp 493 - 509 and 879 - 882.
26. Maslak, P.; Chopra, A. *J. Am. Chem. Soc.* **1993**, 115, 9331.
27. Maslak, P.; Chopra, A.; Moylan, C. R.; Wortmann, R.; Lebus, S.; Rheingold, A. L.; Yap, G. P. A. *J. Am. Chem. Soc.* **1993**, 118, 1471.
28. Beltz, M.; Pfeifer-Fukumura, U.; Kolb, U.; Baumann, W. *J. Phys. Chem. A*. **2002**, 106, 2232.
29. Horii, T.; Abe, T.; Nakao, R. *J. Photochem. Photobiol. A: Chem.* **2001**, 144, 119.
30. Kellmann, A.; Tfibel, F.; Dubest, R.; Levoir, P.; Aubard, J.; Pottier, E.; Guglielmetti, R. J. *Photochem. Photobiol. A: Chem.* **1989**, 49, 63.
31. Lee, D.; Lee, M.; Chung, C.; Lee, W.; Lee, I. *Chem. Lett.* **2003**, 32, 578.
32. Lareginie, P.; Lokshin, V.; Samat, A.; Guglielmetti, R.; Pepe, G. *Chem. Soc., Perkin Trans. 2*. **1996**, 0, 107.
33. Minkin, V. I. *Chem. Rev.* **2004**, 104, 2751.
34. Klajn, R. *Chem. Soc. Rev.* **2014**, 43, 148.

35. Shi, Z.; Peng, P.; Strohecker, D.; Liao, Y. *J. Am. Chem. Soc.* **2011**, 133, 14699.
36. Yang, C.; Khalil, T.; Liao, Y. *RSC. Adv.* **2016**, 6, 85420.
37. Gorner, H. *Phys. Chem. Chem. Phys.* **2001**, 3, 416.
38. Kalisky, Y.; Orlowski, T. E.; Williams, D. J. *J. Phys. Chem.* **1983**, 87, 5333.
39. Bach, H.; Calvert, J. G. *J. Am. Chem. Soc.* **1970**, 92, 2608.
40. Chibisov, A. K.; Gorner, H. *J. Phys. Chem. A.* **1997**, 101, 4305.
41. Raymo, F. M.; Giordani, S. *J. Am. Chem. Soc.* **2001**, 123, 4651.
42. Wojtyk, J. T. C.; Wasey, A.; Xiao, N.; Kazmaier, P. M.; Hoz, S.; Yu, C.; Lemieux, R. P.; Buncel, E. *J. Phys. Chem. A.* **2007**, 111, 2511.
43. Nakashima, T.; Tsuchie, K.; Kanazawa, R.; Li, R.; Iijima, S.; Galangau, O.; Nakagawa, H.; Mutoh, K.; Kobayashi, Y.; Abe, J.; Kawa, T. *J. Am. Chem. Soc.* **2015**, 137, 7023.
44. Takahashi, Y.; Kodama, S.; Ishii, Y. *Organometallics.* **2018**, 37, 1649.
45. Martin, C. J.; Rapenne, G.; Nakashima, T.; Kawai, T. *J. Photochem. Photobio. C: Photochem Rev.* **2018**, 34, 41.
46. Arnaut, L. G.; Formosinho, S. J. *J. Photochem. Photobio. A: Chem.* **1993**, 75, 1.
47. Nunes, R. M. D.; Pineiro, M.; Arnaut, L. G. *J. Am. Chem. Soc.* **2009**, 131, 9456.

48. Abeyrathna, N.; Liao, Y. *J. Photochem. Photobio. A: Chem.* **2017**, 332, 196.
49. Johns, V. K.; Patel, P. K. Hasset, S.; Calvo-Marzal, P.; Qin, Y.; Chumbimuni-Torres, K. Y. *Anal. Chem.* **2014**, 86, 6184.
50. Patel, P. K.; Chumbimuni-Torres, K. Y. *Analyst.* **2016**, 141, 85.
51. Liao, Y. *Acc. Chem. Res.* **2017**, 50, 1956.
52. Liu, F.; Morokuma, K. *J. Am. Chem. Soc.* **2013**, 135, 10693.
53. Prager, S.; Burghardt, I.; Drew, A. *J. Phys. Chem. A.* **2014**, 118, 1339.
54. Kortekaas, L.; Chen, J.; Jacquemin, D.; Browne, W. R. *J. Phys. Chem. B.* **2018**, 122, 6423.
55. Savarese, M.; Raucci, U.; Netti, P. A.; Adamo, C.; Rega, N.; Ciofini, I. *Theor. Chem. Acc.* **2016**, 135:211.
56. Horii, T.; Abe, Y.; Nakao, R. *J. Photochem. Photobio. A: Chem* **2001**, 144, 119.
57. Maurel, F.; Aubard, J.; Rajzmann, M.; Guglielmetti, R.; Samat, A. *J. Chem. Soc., Perkin Trans. 2.* **2002**, 1307.
58. Nakamura, S.; Uchida, K.; Murakami, A.; Irie, M. *J. Org. Chem.* **1993**, 58, 5543.
59. Lee, D-H.; Lee, M.; Chung, C.; Lee, W-H.; Lee, I-J. *Chem. Lett.* **2003**, 578.

60. Delbaere, S.; Bochu, C.; Azaroual, N.; Buntinx, G.; Vermeersch, G. *J. Chem. Soc., Perkin Trans. 2*. **1997**, 1499.
61. Ernsting, N. P.; Dick, B.; Arthen-Engeland, T. *Pure & Appl. Chem.* **1990**, 62, 1483.
62. Becke, A. D. *J. Chem. Phys.* **1993**, 98, 1372.
63. Lee, C.; Yang, W.; Parr, R. G. *Phys. Rev. B*. **1988**, 37, 785.
64. Møller, C.; Plesset, M. S. *Phys. Rev.* **1930**, 46, 618.
65. Tomasi, J.; Mennucci, B.; Cammi, R. *Chem. Rev.* **105**, 8, 2999.
66. Sun, H.; Bozzelli, J. *J. Phys. Chem. A*. **2001**, 105, 9543.
67. Murcko, M. A.; Castejon, H.; Wiberg, K. B. *J. Phys. Chem.* **1996**, 100, 16162.
68. Ross, B. D.; True, N. S.; Matson, G. B. *J. Phys. Chem.* **1984**, 88, 2675.
69. Drakenberg, T. *Tetrahedron Lett.* **1972**, 18, 1743.
70. Rini, M.; Holm, A-K.; Nibbering, E. T. J.; Fidder, H. *J. Am. Chem. Soc.* **2003**, 125, 3028.
71. Kohl-Landgraf, J.; Braun, M.; Özçoban, C.; Gonçalves, D. P. N.; Heclél, A.; Wachtveitl, J. *J. Am. Chem. Soc.* **2012**, 134, 14070.
72. Chibisov, A. K.; Görner, H. *J. Phys. Chem. A*. **1999**, 103, 5211.
73. Aramaki, S.; Atkinson, G. H. *J. Am. Chem. Soc.* **1992**, 114, 438.

74. Sanchez-Lozano, M.; Estéves, C. M.; Hermida-Ramon, J.; Serrano-Andres, L.  
*J. Phys. Chem. A*. **2011**, 115, 9128.